doi:10.3788/gzxb20154409.0906001

基于马赫曾德调制器产生 24 GHz 波段超宽带信号毫米波

汪东,戴博,任栎亲,盛斌,王琦,张大伟
(上海理工大学 光电学院 上海市现代光学系统重点实验室,上海 200093)

摘 要:采用双驱动马赫曾德调制技术生成24GHz波段的超宽带毫米波信号,建立了基于双驱动马赫曾德调制器的超宽带毫米波信号理论模型,并利用理论模型进行实际运算模拟产生了带宽达5.8 GHz的超宽带毫米波信号.研究了毫米波信号的信号质量和带宽.结果表明:通过适当调节毫米波信号发生器的控制信号强度,可以有效抑制产生的毫米波信号中残余振荡和低频成分;控制输入信号的脉冲宽度可实现对生成毫米波信号带宽的灵活调节.该超宽带毫米波信号发生器可用于汽车短程雷达、入侵检测传感器和移动无线电通信等领域.

关键词:信号与信息处理;微波通信;调制技术;微波信号;毫米波
中图分类号:TN29 **文献标识码**:A **文章编号**:1004-4213(2015)09-0906001-5

A Modulation Sheme to Generate 24-GHz-Band Millimeter-wave-band Ultra-wideband Signal by Using Mach Zehnder Modulator

WANG Dong, DAI Bo, REN Li-qing, SHENG Bing, WANG Qi, ZHANG Da-wei
(*Shanghai Key Lab of Modern Optical System, School of Science and Technology, University of Shanghai, Shanghai* 200093, *China*)

Abstract: A single-stage dual-drive Mach Zehnder modulator was employed for the generation of a 24-GHz-band ultra-wide-band signal. A theoretical model for signal generation was derived based on the modulation technique of a dual-drive Mach Zehnder modulator. By the numerical demonstration, an ultra-wideband signal of 5.8 GHz bandwidth was generated. The signal quality and the bandwidth were thoroughly investigated. The results show that residual local oscillation and low-frequency components can be efficiently suppressed if two modulating electrical signals with proper amplitudes are used. The bandwidth of the signal can be flexibly adjusted by simply controlling the pulse width of the input data signal. The millimeter ultra-wideband signal generator is a good candidate for the applications of automotive short-range radar, intrusion detection sensor and mobile radio services.

Key words: Signal processing; Microwave communication; Modulation technique; Microwave signal; Millimeter waves
OCIS Codes: 060.5625; 350.4010; 060.4510

Foundation item: The National Natural Science Foundation of China (No. 61378060), the National Science Instrument Important Project (No. 2013YQ16043903), the Development Program of China (863 Program) (No. 2013AA030602), the Dawn Program of Shanghai Education Commission (No. 11SG44), Scientific Innovation Projects of Shanghai Education Committee (No. 15ZZ071) and Pujiang Project of Shanghai Science and Technology Commission (No. 14PJ1406900)

First author: WANG Dong (1991—), male, M. S. degree, mainly focuses on microwave photonics and optical communications. Email: wangdongonly@163.com
Supervisor(Contact author): ZHANG Da-wei (1977—), male, professor, Ph. D. degree, mainly focuses on optics design, nanofabrication, and optical communication. Email:dwzhang@usst.edu.cn

Received: Mar. 25, 2015; **Accepted**: Jun. 29, 2015

0 Introduction

Ultra-wideband (UWB) radio is a promising technique for next-generation short-distance and high-speed wireless communication, automotive radar and sensing, due to its many advantages including high capacity, multipath robust and low power consumption[1-2]. UWB signal is defined by the U. S. Federal Communications Committee (FCC) as a signal which has a 10 dB bandwidth of more than 0.5 GHz with a power spectral density less than −41.3 dBm/MHz[3-4]. UWB-over-fiber is an efficient technology to significantly expand the coverage of UWB communications by transmitting UWB signals in the optical network[5-6]. Besides the transmission of UWB signals over optical fiber, photonic UWB signal generation and modulation are two preferable approaches for UWB-over-fiber technology to avoid employing unnecessary electrical-to-optical conversion and using expensive broadband RF components[7-8].

The U. S. FCC approves several frequency bands for Millimeter-wave (MMW) systems[9-10]. Among the MMW frequency bands, license-free 24 GHz MMW band is designed for automotive Short-range Radar (SRR) applications, because 24-GHz MMW band has a large bandwidth from 22 to 29 GHz and the large bandwidth is capable for providing a small distance resolution[11-12]. Extensive research efforts have been put into developing photonic UWB communication system within a 24-GHz MMW band[13]. A Dual-Parallel Mach-Zehnder Modulator (DP-MZM), which consists of two Mach-Zehnder Modulators (MZM) in the two arms of a main MZM, was widely used to generate UWB signal[14]. By using a delay interferometer for phase modulation, intensity modulation and harnessing carrier suppression modulation for frequency up-conversion, a pair of polarity-reversed 24 GHz MMW-band UWB monocycles was generated[15]. A polarization modulation based microwave photonic switch was used to generate an UWB signal without low frequency components and residual local oscillation[16-17].

Due to high coherence, high stability and low cost, DD-MZM was driven by two RF signals and controlled by two DC-bias in the two arms of a MZM, was used in the many photonic microwave applications[18]. A versatile waveform generator based on DD-MZM was demonstrated to generate short pulse, triangular, sawtooth and trapezoidal waveforms and FCC-compliment UWB doublet pulse for indoor applications[19]. A DD-MZM has been developed into an optoelectronic oscillator for RF carrier extraction and optical RF signal to baseband down-conversion[20]. An ultra-wideband signal of 5.8 GHz bandwidth is generated and can be adjusted.

1 Theoretical model of the MMW-UWB signal generation

Fig. 1 shows the schematic diagram of the proposed MMW-UWB signal generator. Continuous-wave (CW) light is generated by a laser diode and then fed into a DD-MZM after polarization control. Two RF

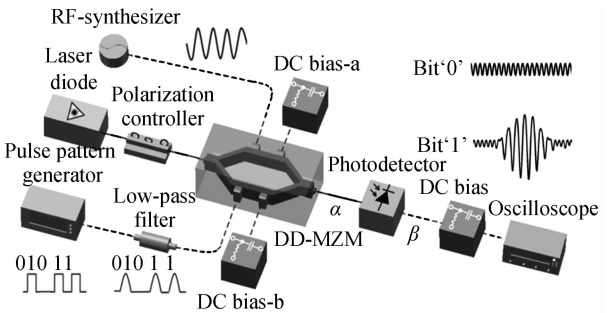

Fig. 1 Schematic diagram of the MMW-UWB signal generator

signals and two DC bias are applied to the two arms of the DD-MZM. The theoretical model of the signal generation is based on the modulation model of the DD-MZM. After the modulation, the output of the DD-MZM can be written as

$$E_{\text{DD-MZM}}(t)=E_{\text{in}}\exp(\mathrm{j}\omega_{\text{c}}t)\left[\exp\left(\mathrm{j}\pi\left(\frac{V_1(t)}{V_{\pi\text{RF}}}+\frac{V_{\text{Bias1}}}{V_{\pi\text{DC}}}\right)\right)+\exp\left(\mathrm{j}\pi\left(\frac{V_2(t)}{V_{\pi\text{RF}}}+\frac{V_{\text{Bias2}}}{V_{\pi\text{DC}}}\right)\right)\right] \tag{1}$$

where E_{in} is the electrical field of the CW light, ω_{c} is optical carrier frequency, $V_{\pi\text{RF}}$ is switching voltage, $V_{\pi\text{DC}}$ is switching bias voltage, V_{Bias1} and V_{Bias2} are the DC bias voltages, and $V_1(t)$ and $V_2(t)$ are the two modulating Radio Frequency (RF) signal.

In the modulation, the two DC bias voltages are set at the minimum transmission point. The two modulating signals are as follows. The RF signal used to modulate the DD-MZM can be expressed as

$$V_1(t)=A\sin(2\pi ft) \tag{2}$$

where A is the amplitude of the RF signal and f is the frequency of the RF signal.

A sequence of Return-to-Zero (RZ) data signal is used to drive the other arm of the DD-MZM after pulse reshaping by using a low-pass filter. The data signal for bit '0' and bit '1' after filtering can be expressed as

$$V_2(t)=\begin{cases}0 & \text{bit '0'}\\ H(t) & \text{bit '1'}\end{cases} \tag{3}$$

where $H(t)$ is the RZ signal after low-pass filtering.

After the DD-MZM, the output electrical field at Point α in Fig. 1 can be written as

$$E_o(t)=\begin{cases} E_{in}\exp(j\omega_c t)\left[\exp\left(j\pi\left(\frac{A\sin(2\pi ft)}{V_{\pi RF}}\right)\right)+1\right] & \text{bit '0'} \\ E_{in}\exp(j\omega_c t)\left[\exp\left(j\pi\left(\frac{A\sin(2\pi ft)}{V_{\pi RF}}\right)\right)+\exp\left(j\pi\frac{H(t)}{V_{\pi RF}}\right)\right] & \text{bit '1'} \end{cases} \quad (4)$$

Then, the modulated signal is sent into a Photodetector (PD) for optical-to-electrical conversion. The output current at point β can be expressed as

$$I(t)=\Re EE^*=\begin{cases} \Re E_{in}^2\left[2+2\cos\left(\frac{A\sin(2\pi ft)}{V_{\pi RF}}\right)\right] & \text{bit '0'} \\ \Re E_{in}^2\left[2+2\cos\left(\frac{A\sin(2\pi ft)}{V_{\pi RF}}\right)+\frac{H(t)}{V_{\pi RF}}\sin\left(\frac{A\sin(2\pi ft)}{V_{\pi RF}}\right)\right] & \text{bit '1'} \end{cases} \quad (5)$$

where $\Re$ is the responsivity of the PD.

In Eq. (5), for both bit '0' and bit '1', there are a DC current and an AC current (cosine term). If the amplitude of the data signal, B, is larger than that of the RF signal, A, the AC term can be neglected, remaining the DC term for both data bit '0' and '1' and a *sine* term with the envelop of $H(t)$ for bit '1', which is the generated MMW signal with the center frequency of f. Practically, the DC term could be removed by using a DC-bias. To obtain a background-free MMW signal, residual local oscillation components and low-frequency components should be weakened by adjusting the ratio between the amplitudes of the data signal and the RF signal and setting a proper DC-bias.

2 Demonstration of MMW-UWB signal generation

Based on the theoretical model, the generation of MMW-UWB signal is demonstrated. The system parameters are set as follows. A Continuous-wave (CW) laser source is used. The center wavelength of the input CW light is 1 550 nm. Then, a polarization controller is followed to adjust the polarization of the light to fit the modulation. The switching voltage, $V_{\pi RF}$, and the switching bias voltage, $V_{\pi DC}$, are 4 V. The frequency of the RF signal is 25.5 GHz, which is the center of the 24 GHz-band. A second-order Butterworth low-pass filter is used to reshape the data signal. Fig. 2 illustrates the waveform of the data signal before and after the filter for data bit '1'. The red dashed line represents RZ data signal, blue solid line represents the signal after filtering, and the inset represents the frequency response of the second-order Butterworth low-pass filter. The frequency response of the filter is in the inset. The cutoff frequency of the filter is 3.5 GHz. The input RZ data signal has the pulse width of 160 ps. After filtering, the pulse width (full width at half maximum) is almost unchanged. The amplitudes of the data signal and the RF signal are 10 V and 0.5V, respectively. The ratio between the amplitudes of the data signal and the RF signal, B/A, is 20. Both V_{Bias1} and V_{Bias2} are set to 0 V. In practice, to avoid the bias drifting, the DC bias could be connected to the ground. After modulation, the optical signal is converted to an electrical signal by using a photodetector. The photodetector has the bandwidth of 50 GHz. The responsivity is 1 A/W.

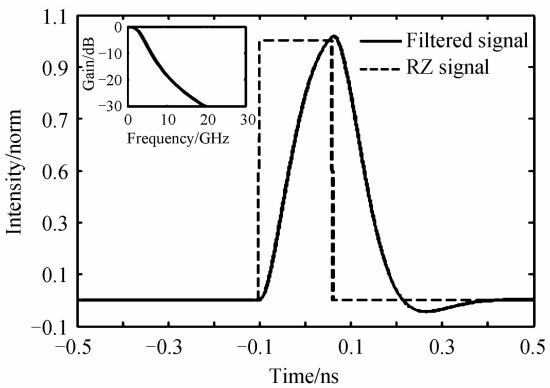

Fig. 2 Waveform of the calculated data signal for bit '1'

Fig. 3 shows the normalized waveforms of the generated MMW-UWB signals for data bit '0' and bit '1', respectively. The MMW-UWB signals have equal amplitudes above and below the DC level. Since B/A ratio is high, the AC term is suppressed and the residual local oscillation is diminished. In the corresponding power spectrum, as shown in Fig. 4, the generated MMW-UWB signal is centered at 25.5 GHz and has a 10 dB bandwidth of 5.8 GHz. The red dashed line represents the FCC-specified spectral mask. The MMW - UWB signal conforms to the FCC -

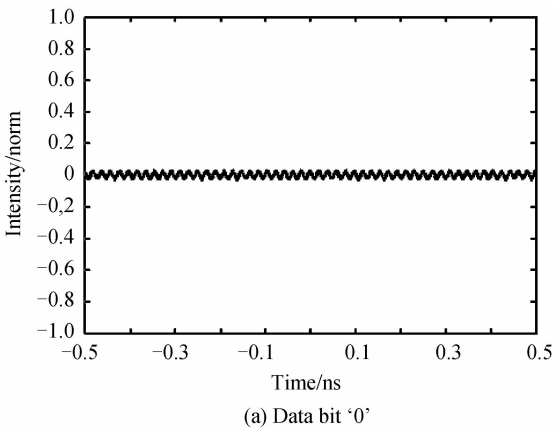

(a) Data bit '0'

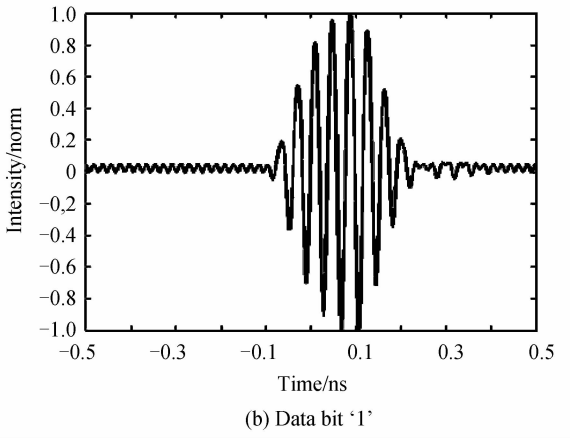

Fig. 3 The normalized waveforms of the generated MMW-UWB signals

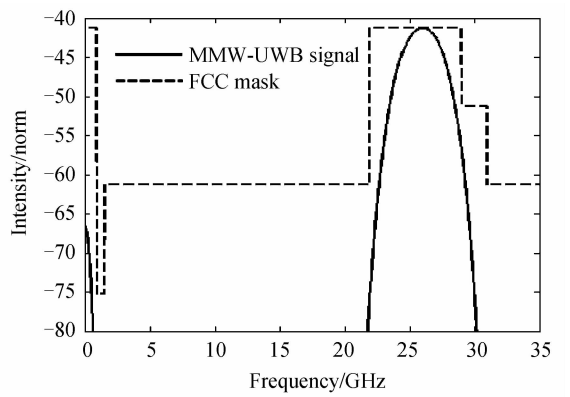

Fig. 4 The power spectrum of the generated MMW-UWB signals

specified spectral mask very well. The low-frequency components are weak compared with the target MMW-UWB signal.

3 Influence over the generation of MMW-UWB signal

According to the theoretical model, it is found that the generation of the MMW-UWB signal is affected by the input signals. As predicted previously, the ratio between the amplitudes of the data signal and the RF signal, B/A, has the influence over the signal quality of the generated UWB-MMW signal. To investigate the influence of the two modulating electrical signals over the UWB signal generation, the ratio between the amplitudes of the data signal, B, and the RF signal, A, is changed. In the analysis, the frequency of the RF signal, f, is 25.5 GHz. Both the switching voltage, $V_{\pi RF}$, and the switching bias voltage, $V_{\pi DC}$, are 4V. The two DC bias voltages are 0V.

Fig. 5 shows the relationship of the B/A ratio and the suppression effect of the residual local oscillation. The ratio between the amplitudes of the target MMW-UWB signal to the residual local oscillation is from 10 to 37, when B/A ratio is set from 5 to 20. As shown in the inset, serious residual local oscillation can be observed in the MMW-UWB signal generated by small B/A ratio, while the MMW-UWB signal generated by large B/A ratio has equal amplitudes above and below DC level and weak residual local oscillation, because the amplitude of the data signal becomes a dominant factor and strengthens the target signal comparing to the residual local oscillation.

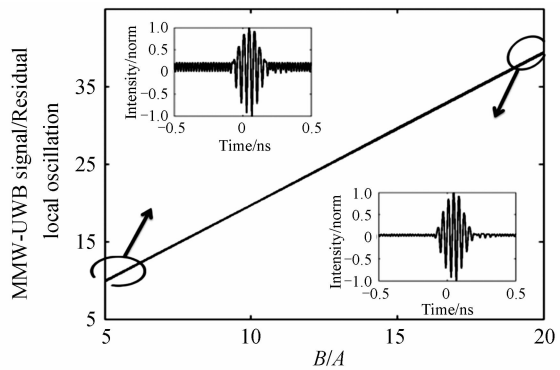

Fig. 5 The relationship of the B/A ratio and the suppression effect of the residual local oscillation

In addition, the bandwidth of the MMW-USWB signal is of great importance. The influence over the bandwidth of the generated MMW-UWB signal is investigated. B/A ratio is kept at 20. The pulse width of the input data signal is changed from 120 ps to 200 ps. Fig. 6 illustrates the relationship between the

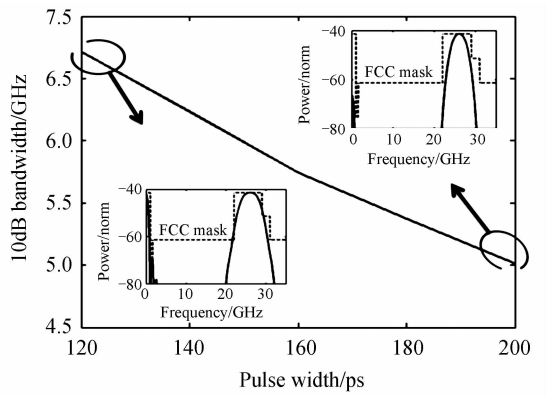

Fig. 6 The pulse width of the input data signal versus the 10 dB bandwidth of the generated MMW-UWB signal

pulse width of the input data signal and the 10 dB bandwidth of the generated MMW-UWB signal. The power spectra of the generated signals for the input pulse width of 120 ps and 200 ps are shown in the inset. The 10 dB bandwidth of the MMW-UWB signal shrinks from 6.7 GHz to 5 GHz with the increase of the pulse width of the data signal, because the pulse width of the generated MMW-UWB increases accordingly. In other words, a short data pulse contributes to a wide-bandwidth MMW signal. Furthermore, the signal generated by a wide pulse has

fewer low-frequency components. Thus there is a compromise between wide bandwidth and good signal quality. To obtain the MMW-UWB signal with wide bandwidth and good quality, a proper duty cycle of the input RZ signal should be selected.

4 Conclusion

A 24-GHz-band MMW-UWB signal generation scheme is proposed by employing a single-stage DD-MZM. A theoretical model is built for the demonstration and analysis. In the demonstration, a MMW-UWB signal with the bandwidth of 5.8 GHz is generated at 25.5 GHz. The generated MMW-UWB signal conforms to the FCC regulation well. We have found that the residual local oscillation and the low-frequency components of the generated signal could be efficiently suppressed by increasing the ratio between the amplitudes of the input data signal and the RF signal. Besides, the MMW-UWB signal with wide bandwidth can be obtained by using the input data signal of short pulse width. The proposed MMW-UWB signal generation scheme would be a good candidate for various MMW-UWB applications.

References

[1] AIELLO G R, ROGERSON G D. Ultra-wideband wireless systems[J]. *IEEE Microwave Magazine*, 2003, **4**(2): 36-47.

[2] DOMENICO P, WALTER H. Ultra-wideband radio technology: potential and challenges ahead [J]. *IEEE Communications Magazine*, 2003, **41**(7): 66-74.

[3] ZHOU Ming-tuo, SHARMA A B, ZHANG Jian-guo, *et al*. A novel configuration for millimeter-wave radio-over-fiber (ROF) transmission systems with remote local-oscillator delivery[J]. *Acta Photonica Sinica*, 2006, **35**(11): 1725-1729.

[4] GHAVAMI M, MICHAEL L B, KOHNO R. Ultra wideband signals and systems in communication engineering[M]. Wiley-IEEE Press, West Sussex, 2004.

[5] HU Shan-Mei, CHEN Lin. A radio over fiber system with frequency sextuple optical millimeter-wave generation carrying OFDM signal utilizing phase modulator[J]. *Acta Photonica Sinica*, 2010, **39**(4): 699-703.

[6] ZENG Fei, YAO Jian-ping. An approach to ultrawideband pulse generation and distribution over optical fiber[J]. *IEEE Photonics Technology Letters*, 2006, **18**(7): 823-825.

[7] JUAN Yu-shan, LIN Fan-yi. Demonstration of ultra-wideband (UWB) over fiber based on optical pulse-injected semiconductor laser[J]. *Optics Express*, 2010, **18**(9): 9664-9670.

[8] YIN Xiao-li, HAN Jing-jing, XU Can, *et al*. Optics assisted envelope detection of PMM-UWB employing phase/intensity modulation [J]. *Acta Photonica Sinica*, 2015, **44**(2): 206001-.

[9] ABRAHA S, OKONKWO C, TANGDIONGGA E, *et al*. Power-efficient impulse radio ultrawideband pulse generator based on the linear sum of modified doublet pulses[J]. *Optics Letters*, 2011, **36**(12): 2363-2365.

[10] YU Xian-bin, MONROY I T. Distribution of photonically generated 5 Gbits/s impulse radio ultrawideband signals over fiber[J]. *Optics Letters*, 2011, **36**(6): 810-812.

[11] CHANG Qing-jiang, TIAN Yue, YE Tong, *et al*. A 24-GHz ultra-wideband over fiber system using photonic generation and frequency up-conversion [J]. *IEEE Photonics Technology Letters*, 2008, **20**(19): 1651-1653.

[12] LI Wei, WANG LI-xian, ZHENG Jian-yu, *et al*. Photonic MMW-UWB signal generation via DPMZM-based frequency up-conversion[J] *IEEE Photonics Technology Letters*, 2013, **25**(19): 1875-1878.

[13] LI Jing, NING Ti-gang, PEI Li, *et al*. Simulation analysis of a photonic ultrawideband pulse generator by using a dual-parallel mach-zehnder modulator[J]. *Optical Engineering*, 2011, **50**(10): 105007.

[14] ZHANG Fang-zheng, PAN Shi-long. Background-free millimeter-wave ultra-wideband signal generation based on a dual-parallel mach-zehnder modulator[J]. *Optics Express*, 2013, **21**(22): 27017-27022.

[15] YU Yuan, DONG Jian-ji, LI Xiang, *et al*. Photonic generation of millimeter-wave ultra-wideband signal using phase modulation to intensity modulation conversion and frequency up-conversion[J]. *Optics Communications*, 2012, **285**(7): 1748-1752.

[16] DU Yuan-xin, ZHENG Jian-yu, WANG Li-xian, *et al*. Widely-tunable and background-free ultra-wideband signals generation utilizing polarization modulation-based optical switch[J]. *IEEE Photonics Technology Letters*, 2013, **25**(4): 335-337.

[17] WANG Li-xian, LI Wei, ZHENG Jian-Yu, *et al*. High-speed microwave photonic switch for millimeter-wave ultra-wideband signal generation[J]. *Optics Letters*, 2013, **38**(4): 579-581.

[18] DAI Bo, GAO Zhen-sen, WANG Xu, *et al*. Versatile waveform generation using single-stage dual-drive mach-zehnder modulator[J]. *Electronics Letters*, 2011, **47**(5): 336-338.

[19] DAI Bo, GAO Zhen-sen, WANG Xu, *et al*. Generation of versatile waveforms from CW light using a dual-drive mach-zehnder modulator and employing chromatic dispersion[J]. *Journal of Lightwave Technology* 2013, **31**(1): 145-151.

[20] TANG Zhen-zhou, ZHANG Fang-zheng, PAN Shi-long. Photonic microwave downconverter based on an optoelectronic oscillator using a single dual-drive mach-zehnder modulator [J]. *Optics Express*, 2014, **22**(1): 305-310.